Vesicle deformation by microtubules: A phase diagram

Virginie Emsellem, Olivier Cardoso, and Patrick Tabeling
Laboratoire de Physique Statistique de l'École Normale Supérieure, Associé au Centre National de la Recherche Scientifique et aux Universités Paris 6 et Paris 7, 24 rue Lhomond, F-75231 Paris Cedex 05, France
(Received 6 April 1998)

The experimental investigation of vesicles deformed by the growth of encapsulated microtubules shows that the axisymmetric morphologies can be classified into ovals, lemons, ϕ, cherries, dumbbells, and pearls. A geometrical phase diagram is established. Numerical minimization of the elastic energy of the membrane reproduces satisfactorily well the observed morphologies and the corresponding phase diagram.
[S1063-651X(98)01910-2]

PACS number(s): 87.22.Bt

The description of cells in terms of a hierarchy of interacting systems has brought about a better understanding of some mechanisms of their behavior, together with questions about the physics of biological objects. In particular, the cytoskeleton is made of polymers that have an interesting mechanical behavior, at a scale inaccessible to common mechanical systems. In this paper we are interested in microtubules, which are thin, rigid, dynamical filaments [1], with a growth time of the order of minutes. *In vivo*, they play an important role in intracellular communication and they also have been shown to be crucially related to cell motility through the centering of the centrosome [2]. When the cell membrane is modified so as to be less rigid (depolymerization of cortical actin) [3], it has been observed that long, thin extensions of the membrane develop, giving rise to morphologies resembling the letter ϕ. This phenomenon is due to the action of microtubules growing across the cell and deforming the membrane while being brought together into a bundle. The same effect has been observed in simpler systems [4,5] where microtubules are forced to polymerize in phospholipid vesicles. In particular, it has been shown theoretically in Ref. [5] that the ϕ shape was more stable than an oval for long enough microtubules. It is tempting to generalize this approach and attempt to establish a phase diagram, which would classify all the experimentally observable morphologies, on a physical basis. This is the aim of this paper.

In the experiments, tubulin is purified from porcine brain by three cycles of cold/hot centrifugation and then by elimination of associated proteins by an ion exchange (phosphocellulose) column [6]. The final solution is 4 mg/ml tubulin in a buffer composed of 100 m*M* pipes (piperazine-*N*,*N*′-bis[2-ethansulfonic acid]), 2 m*M* EGTA (ethylene glycol-bis[β-aminoethyl ether] *N*,*N*,*N*′,*N*′-tetraacetic acid), 2 m*M* $MgSO_4$, 1 m*M* GTP (guanosine 5′-triphosphate) at *p*H=6.9. The phospholipids used here are synthetic: It is a mixture of 40% DOPS (1,2-dioleoyl-*sn*-glycero-3-[phospho-*L*-serine], which has a negatively charged head and prevents tubulin from sticking to the membrane) and 60% DOPC (1,2-dioleoyl-*sn*-glycero-3-phosphocholine, which has a neutral head); they are in solution in chloroform at a concentration of 10 mg/ml. Their critical temperature is below 0 °C, which allows the phospholipid film to be in a fluid phase while tubulin is unpolymerized. 25 μl of this solution are deposited on the bottom of a glass tube and the solvent is evaporated by a nitrogen flux and then by vacuum desiccation for 2 h. This lamellar phase is then rehydrated during 2 h on ice by 25 μl of the tubulin solution (the final tubulin concentration is $c=1.3$–4 mg/ml). Some experiments are performed with 1% rhodamine-labeled tubulin (purchased from Cytoskeleton, Denver) added to the tubulin in order to check by fluorescence the location of the microtubules. The vesicle solution is pipetted out of the tube and left on ice for another hour in order to allow for possible reorganization of the membranes. Centrifugation for 1 min at 100*g* follows, which reassembles in the pellet the high lamellarity vesicles or phospholipid aggregates. 15 μl of the supernatant are diluted 5 times in NaCl, 150 m*M*: The osmolarities of the inner and outer solutions are the same, but the observation is made easier owing to the increase of the contrast of the vesicles under the microscope and their sedimentation at the bottom of the observation chamber. This solution, transferred into a glass observation chamber made of a microscope slide and coverslip spaced and sealed by a 100 μm thick Parafilm, is observed by phase contrast or fluorescence microscopy (Leica) on a homemade water flow thermalized stage, the temperature of which is set to $22\,^{\circ}\mathrm{C}<T<40\,^{\circ}\mathrm{C}$. A charge couple device video camera, for phase contrast, or an intensified tube camera (LHESA, Cergy-Pontoise, France), for fluorescence, is adapted on the microscope and the pictures are recorded on a video tape and sent to a computer for processing. Homemade image processing software based on NIH IMAGE [7] allows us to measure the geometrical parameters of the vesicles (surface, volume, etc.), assuming the object is axisymmetric ''by portions.''

A few minutes after the solution is set to the operating temperature *T*, the microtubules grow inside the vesicles and eventually deform a reasonable proportion of the liposomes. For unclear reasons, the best results (highest ratio of the number of deformed vesicles to the total number of vesicles) are obtained in a narrow range around $T=22\,^{\circ}\mathrm{C}$ and $c=2.5$ mg/ml. Depending on the ratio of the initial radius R_0 of the vesicle to the length L of the microtubule bundle, one can obtain different equilibrium vesicle shapes. The use of the term ''equilibrium shape'' is justified here because the growth velocity of microtubules is micrometers per seconds [1], while the lowest thermal fluctuation frequency of a fluid vesicle of typically 10 μm is above 1 Hz [8]. To check that these membrane deformations were not one aspect of liposome polymorphism, some experiments were performed with rhodamine-labeled tubulin and revealed that tubulin was polymerized as microtubules in the arms of the vesicles, as shown in Fig. 1. In all cases, the high rigidity of the cylin-

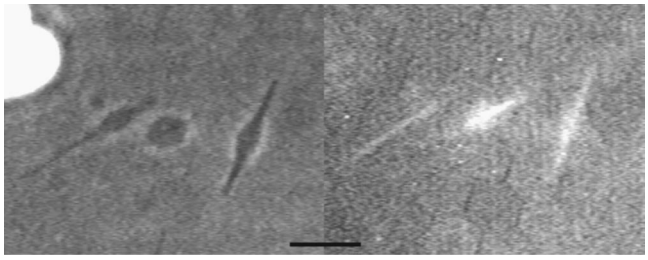

FIG. 1. Pictures of three vesicles containing rhodamine-labeled tubulin deformed in ϕ shapes as seen in phase contrast (left) and fluorescence (right) microscopy. The bar is 10 μm.

drical parts of the deformed vesicles allows one to detect without ambiguity the presence of microtubules. All the axisymmetric final shapes we have observed are shown in Fig. 2. They have been called oval, lemon, cherry, ϕ, dumbbell, and pearls. Other, marginal, nonaxisymmetric, starlike shapes have also been observed, but we do not discuss them here.

From an overall look at the morphologies, two constituting subparts can be exhibited: a variable length, thin, cylindrical piece (the arm), which contains a small fraction of the volume enclosed by the vesicle, and a round piece (the body), which contains most of the volume at hand. All the morphologies are built from these subparts: The oval is armless and the lemon has precursor arms. The ϕ, cherry, and dumbbell have one or two arms with one or two bodies. This is how the vesicle accommodates a fixed volume with a long rod inside. Most ϕ are asymmetric, both arms being of different lengths; the cherry corresponds to the extreme case where one of the arms is absent. From a mechanism that is possibly related to a pearling instability [9], the body can split into two parts, giving rise to dumbbells. ''Higher-order'' shapes (with more arms and more bodies) have been observed, but they are extremely rare.

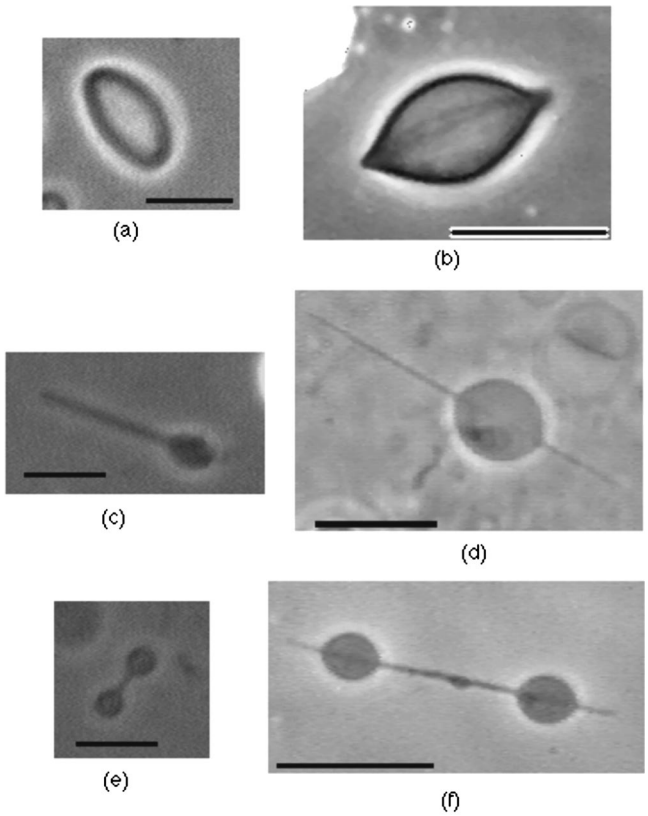

FIG. 2. Photographs of experimental shapes. (a) oval, (b) lemon, (c) cherry, (d) ϕ, (e) dumbbell, and (f) pearls. Pictures are in phase contrast microscopy. The bars are 10 μm.

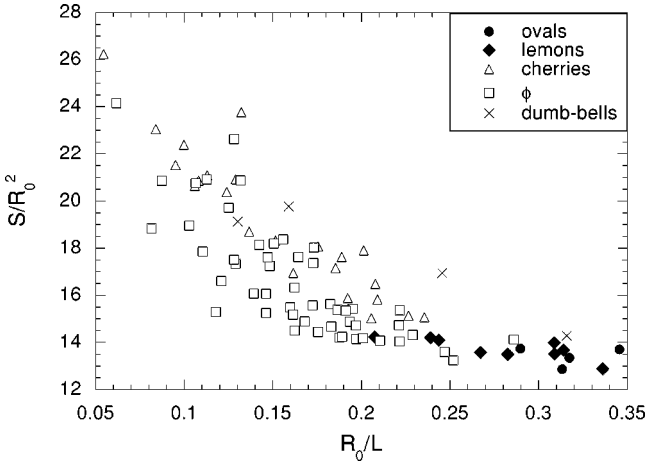

FIG. 3. Experimental phase diagram of morphologies classified through the parameters R_0/L and S/R_0^2.

We propose here to perform a classification of the morphologies of the vesicles using two geometrical parameters R_0/L and S/R_0^2, where S is the surface of the equilibrium vesicle, L the length of the microtubule(s), and R_0 the radius of the equivalent spherical vesicle (whose volume is $4\pi R_0^3/3$). The phase diagram obtained this way is plotted in Fig. 3. The values of S/R_0^2 are bounded down by 4π (sphere) and lie well below the cylindrical limit $2\pi(R_0/L)^{-1}$. This diagram separates the above-mentioned types and shows that before a transition located roughly at $R_0/L=0.23$ armed shapes are dominant, while round shapes are the most common for higher R_0/L. In practice, the parameter R_0/L thus seems a useful tool to distinguish between armed and nonarmed morphologies. Nonetheless, the cherries and ϕ are not separated in this phase diagram. A closer examination suggests that there is another transition from lemons to ovals near $R_0/L=0.3$, but data are lacking to have strong experimental evidence of this transition. The dumbbells are rare and are found in any part of the phase diagram.

Three of the morphologies have been reported by Fygenson *et al.* [5]: ovals, lemons, and ϕ. They explain the existence of the ϕ by energetic considerations, showing that, for large enough R_0/L, a ϕ is more stable than an oval. We generalize these investigations by performing a numerical minimization of the Helfrich energy of the membrane [10] by simulated annealing [11]. For a membrane, this energy is the sum of two terms $E=E_H+E_S$, bending (E_H) and stretching (E_S). E_H is given by

$$E_H=\frac{1}{2}k_c\int\left(\frac{1}{R_1}+\frac{1}{R_2}\right)^2 dS,$$

where k_c is the bending modulus and R_1 and R_2 are the main curvature radii. This choice is justified by the following considerations [10]: The membranes being symmetric, we neglect the spontaneous curvature of the bilayer; moreover, the

Gaussian curvature is known to be a topological invariant, so that its contribution is also neglected. Moreover, it is useful to keep in mind that the bending energy of a sphere is $8\pi k_c$, independent of its radius. Concerning E_S, Evans and Rawicz showed experimentally [12] that two regimes appear when a vesicle is stretched. Let S be the area of the vesicle and S_0 its initial (unstretched) area; when the relative extension $\alpha = (S-S_0)/S_0$ is small, the behavior of the membrane is entropic while, under sufficient tension, it turns to direct expansion. For DMPC (1,2-dimyristoyl-*sn*-glycero-3-phosphocholine), which we believe has a behavior comparable to DOPS/DOPC, the threshold is reported to be located at $\alpha = \alpha_c \approx 0.02$. As can be computed from Fig. 3, our experimental values for α vary from 0.05 for ovals to 1 for ϕ and cherries, which clearly locates our vesicles in the expansion regime [13]. The stretching energy is then given by

$$E_S = \frac{1}{2} k_s \frac{(S-S_0)^2}{S_0},$$

with k_s the stretching modulus. Within this framework, a deformed vesicle is characterized by its geometrical parameters R_0, S, L, and its energetic parameters k_s and k_c; therefore, a dimensional analysis shows that the full problem depends only on three dimensionless variables R_0/L, S/R_0^2, and $k_s R_0^2/k_c$. The experimental diagram of Fig. 3 thus incorporates two of the full set of dimensionless parameters. The values we use for k_s and k_c are such that $k_s R_0^2/k_c$ lies in the experimental range [14].

Schematically, we assume in the numerics that the vesicles are constrained to have a fixed volume $4\pi R_0^3/3$ and that they adapt so as to contain a rigid rod of length L. Moreover, we impose a symmetry of revolution around this rod. Numerically, the membrane shape is modeled by a set of typically 80 points with discrete distances from the axis of revolution. With these constraints, the energy E is minimized. The method allows us to determine the equilibrium axisymmetric shapes of vesicles that accommodate a microtubule of length L, provided a wide range of initial conditions is considered. The calculation shows that the equilibrium shapes are, for R_0/L decreasing from 0.5 to 0, the oval, the lemon, and then, simultaneously present in the same range of R_0/L, the ϕ (with indifferent position of the round part) and the cherry. By carefully choosing the initial condition of the calculation, it appears that another shape is stable: the dumbbell. Such shapes are presented in Fig. 4. Imposing more symmetries to the initial conditions leads to many-body equilibrium shapes, which are unlikely since they correspond to much higher energy levels. We have thus been able to reproduce all the observed axisymmetric morphologies. Although dumbbells are stable equilibrium shapes in the sense that they correspond to an energy well, their energy is higher than that of a ϕ with the same R_0 and L by a factor that can reach 10^4 in our numerical simulations. A simple argument can account for such orders of magnitude by considering mainly the nearly spherical parts of the vesicles: In the ϕ, nearly all the volume V is enclosed in a sphere of surface S, leading to a bending energy $E_H \approx 8\pi k_c$ and stretching energy $E_S \approx k_s (S-S_0)^2/2S_0$; for the dumbbell, the same volume V is split into two spheres and now occupies a surface $2^{1/3}S$, so

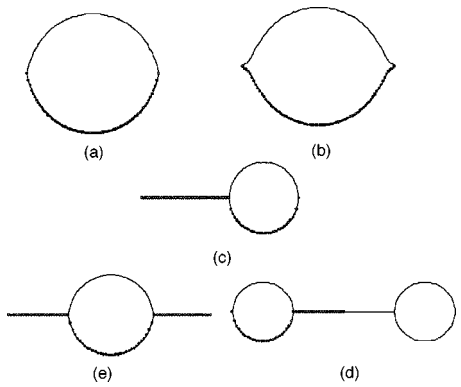

FIG. 4. Numerical shapes resulting from energy minimization: (a) oval ($R_0 = 0.24$ μm, $L = 0.51$ μm), (b) lemon ($R_0 = 0.24$ μm, $L = 0.58$ μm), (c) cherry ($R_0 = 4.1$ μm, $L = 18$ μm), (d) ϕ ($R_0 = 2.3$ μm, $L = 12$ μm), and (e) dumbbell ($R_0 = 4.0$ μm, $L = 6.9$ μm). The small dots are the computation points.

that $E_H' \approx 2E_H$ while $E_S' \approx k_s(2^{1/3}S - S_0)^2/2S_0 \approx E_S\{1 + [(2^{1/3}-1)S/(S-S_0)]^2\}$. This additional term can reach high values, making the dumbbell an unlikely morphology. Because the system has to jump a high-energy barrier (of order $10^3 k_c \approx 4\times 10^4 k_B T$ in the numerics) to initially pinch the vesicle, the dumbbells are extremely rare experimentally; this argument can be extended to pearls.

We now turn to the four most stable morphologies: ovals, lemons, ϕ, and cherries. We have so far seen that they could be geometrically classified into two types. The numerics provide additional energetic considerations that enhance the distinction; they are based on the relative weights of E_H and E_S. The armless morphologies (ovals and lemons), which hardly deviate from a sphere, have a bending energy that is nearly constant (independent of their volume) and a small E_S. On the contrary, for the armed morphologies (ϕ and cherries), the contributions of E_H and E_S to the total energy are equivalent. This analysis in terms of energy is useful to understand the behavior of the vesicles as an exchange of the dominant energy (the one the system takes the more benefit in minimizing).

We also performed a geometrical phase diagram analysis on the numerical data, the result of which is plotted in Fig. 5.

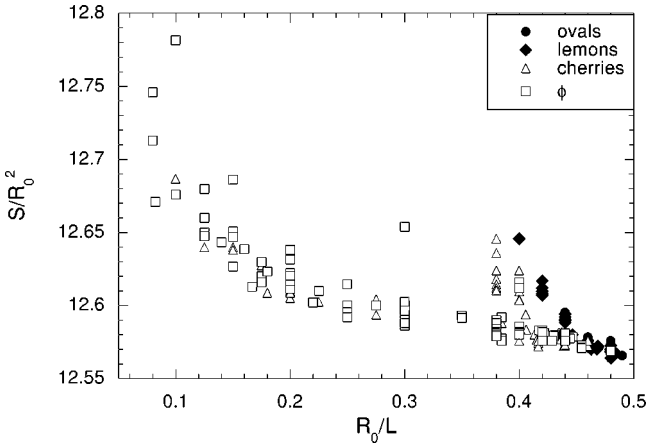

FIG. 5. Same phase diagram of morphologies as in Fig. 3 but with numerical vesicles.

The qualitative agreement with Fig. 3 is good: There is a well-defined transition from round to armed shapes, independent of $k_s R_0^2/k_c$ in the range we have considered. The region containing ovals can be qualitatively reproduced by a simple geometrical model, considering that the ovals lie between ellipsoids and spherical shells. This is also true in the experimental diagram, but fails to explain the transition from round to armed shapes, for which energetic considerations are necessary. In both diagrams, experimental as well as numerical, one can see that cherries and ϕ coexist in the same range of R_0/L. Both are stable equilibrium shapes, although the numerics show that the cherries are slightly less energetic (the energy difference between the two morphologies is, however, small: roughly 20% or $k_c/20$, $\approx 2k_BT$ in absolute value). In the numerics, the evolution towards a cherry rather than a ϕ is sensitive to the initial conditions used for minimization: The location of the body of the ϕ is energetically indifferent; however, should it be close to one end of the rod, the system would easily evolve towards the cherry. If, on the contrary, the body is centered, it remains in the energy well corresponding to a ϕ. In the simulated annealing, we start with a fixed L and an oval vesicle and ''thermal energy'' is added to the membrane for it to explore the parameter space and find the most stable equilibrium; in the experiments, the microtubules grow and tend to push equally on both sides of the vesicle. Such different behaviors might explain why ϕ are more common experimentally than numerically. It is clear anyhow that, given the small energy difference between ϕ and cherries, the robustness of the proportion of cherries remains to be assessed since it may also depend on numerical details [15]. In order to test the robustness of the numerical approach, we have also performed simulations considering the full form of the energy, i.e., including both the expansion and the entropic regimes, and using plausible values for the physical quantities at hand [12]. For a certain range of parameters, these simulations show that the equilibrium shapes mostly stand in the expansion regime, as in the experiments. In all cases, the phase diagrams we obtain are extremely similar to that of Fig. 5; this indicates that such a diagram is fairly robust and moreover suggests that it may be of relevance for a broad class of physical situations.

In this paper we have considered the problem of the deformation of a fluid membrane by a rigid rod, which is experimentally achieved by growing microtubules in a phospholipidic vesicle (its biological relevance is not tackled here). What we have shown is that there exists other morphologies than what had been reported so far: the cherry and the dumbbell. These shapes are well explained by simply considering the Helfrich equilibrium energy of the membrane, regardless of the dynamics of the microtubules. The calculations show that other axisymmetric shapes are extremely unlikely on such a system. All the morphologies are classified in a phase diagram, the experiments showing that the morphological class of the vesicle (with or without arms) mainly depends on the aspect ratio L/R_0 of the vesicle, which is qualitatively well reproduced by the numerics.

We acknowledge Albrecht Ott, Michel Bornens, Simon Holmes, Mohammed Moudjou, Daniel Lévy, Daniel Riveline, Jean-Jacques Lacapeyre, and Deborah Fygenson for experimental help and Jacques Prost, Frank Jülicher, Eric Karsenti, and Stanislas Leibler for interesting discussions.

[1] T.J. Mitchinson and M. Kishner, Nature (London) **312**, 237 (1984).
[2] M. Ueda, R. Gräf, H. MacWilliams, M. Schliwa, and U. Euteneuer, Proc. Nat. Acad. Sci. USA **94**, 9674 (1997).
[3] E. Bailly, C. Celati, M. Bornens, Exp. Cell Res. **196**, 287 (1991).
[4] H. Miyamoto and H. Hotani, Adv. Biophys. **26**, 135 (1990).
[5] D.K. Fygenson, J.F. Marko, and A. Libchaber, Phys. Rev. Lett. **79**, 4497 (1997).
[6] D. Kuchnir Fygenson, Ph.D. thesis, Princeton University, 1995 (unpublished).
[7] Public domain NIH IMAGE program, developed at the U.S. National Institutes of Health and available from the Internet by anonymous ftp from zippy.nimh.nih.gov or on floppy disk from the National Technical Information Service, Springfield, Virginia, part No. PB95-500195GEI. Both adapted source code and compiled application for MacOS are available at http://www.lps.ens.fr/ cardoso
[8] M.B. Schneider, J.T. Jenkins, and W.W. Webb, J. Phys. (Paris) **45**, 1457 (1984).
[9] R. Bar-Ziv and E. Moses, Phys. Rev. Lett. **73**, 1392 (1994).
[10] W. Helfrich and R.M. Servuss, Nuovo Cimento D **3**, 137 (1984).
[11] W.H. Press, S.A. Teukolsky, W.T. Vetterling, and B.P. Flannery, *Numerical Recipes in C* (Cambridge University Press, Cambridge, 1992).
[12] E.A. Evans and W. Rawicz, Phys. Rev. Lett. **64**, 2094 (1990).
[13] Note that the experimental surface and volume are probably slightly overestimated because of the limitations of the pixel size and microscope resolution, especially in the arms. However, given the estimated uncertainty on α (of order 20%), the conclusion remains.
[14] The experimental values are $k_s = 0.1 - 0.2$ J/m^2 and $k_c = 1.6 \times 10^{-19}$ J, respectively, measured in Ref. [12] and by Song and Waugh, J. Biomech. Eng. **112**, 235 (1990).
[15] F. Jülicher (private communication).